Cell

Dual Action of ATP Hydrolysis Couples Lid Closure to Substrate Release into the Group II Chaperonin Chamber

Nicholai R. Douglas,[1] Stefanie Reissmann,[1,4] Junjie Zhang,[3] Bo Chen,[2] Joanita Jakana,[3] Ramya Kumar,[1] Wah Chiu,[2,3] and Judith Frydman[1,*]
[1]Department of Biology and BioX Program, Stanford University, Stanford, CA 94305-5020, USA
[2]Program in Structural and Computational Biology and Molecular Biophysics
[3]National Center for Macromolecular Imaging
Baylor College of Medicine, Houston, TX 77030, USA
[4]Present address: MPI for Terrestrial Microbiology, Marburg D-35043, Germany
*Correspondence: jfrydman@stanford.edu
DOI 10.1016/j.cell.2010.12.017

SUMMARY

Group II chaperonins are ATP-dependent ring-shaped complexes that bind nonnative polypeptides and facilitate protein folding in archaea and eukaryotes. A built-in lid encapsulates substrate proteins within the central chaperonin chamber. Here, we describe the fate of the substrate during the nucleotide cycle of group II chaperonins. The chaperonin substrate-binding sites are exposed, and the lid is open in both the ATP-free and ATP-bound prehydrolysis states. ATP hydrolysis has a dual function in the folding cycle, triggering both lid closure and substrate release into the central chamber. Notably, substrate release can occur in the absence of a lid, and lid closure can occur without substrate release. However, productive folding requires both events, so that the polypeptide is released into the confined space of the closed chamber where it folds. Our results show that ATP hydrolysis coordinates the structural and functional determinants that trigger productive folding.

INTRODUCTION

Achieving correct protein folding is critical for cellular health and viability. Failure to fold and maintain protein homeostasis is associated with a growing number of diseases (Hartl and Hayer-Hartl, 2009; Powers et al., 2009). Accordingly, cell viability is dependent on a class of proteins called molecular chaperones, which bind nonnative proteins and facilitate their folding (Bigotti and Clarke, 2008; Frydman, 2001; Hartl and Hayer-Hartl, 2009; Spiess et al., 2004). Among these, the group II chaperonins found in eukaryotic cells and archaea have a unique ring-shaped structure that determines their functional characteristics (Bigotti and Clarke, 2008; Gómez-Puertas et al., 2004; Spiess et al., 2004). For instance the eukaryotic chaperonin TRiC/CCT assists the folding of ~10% of newly translated proteins, including essential cytoskeletal proteins, cell-cycle regulators, and tumor suppressors (Thulasiraman et al., 1999; Yam et al., 2008). Intriguingly, many of its substrates, such as actin, cannot be folded by other chaperone systems (Spiess et al., 2004), suggesting that TRiC possesses unique mechanistic features absent from other chaperones.

Group II chaperonins are large complexes consisting of two stacked rings of eight (or less frequently nine) subunits each (Bigotti and Clarke, 2008; Gómez-Puertas et al., 2004; Spiess et al., 2004). Individual subunits are generally different, ranging from one to four in archaea, to eight different subunits for TRiC/CCT. The general subunit architecture is conserved across group II chaperonins. Each subunit consists of an equatorial, ATP-binding domain, an intermediate hinge domain, and an apical domain, which contains the substrate-binding sites; a flexible protrusion extends from the apical domain and acts as a built-in lid. ATP binding and hydrolysis drives group II chaperonins through a conformational cycle that is not well understood. In the absence of nucleotide, the lid-containing segments are open, and the complex binds substrate. The open-state structures of TRiC/CCT and an archaeal chaperonin from *Methanococcus maripaludis* are remarkably similar (Booth et al., 2008; Pereira et al., 2010; Zhang et al., 2010). Incubation with hydrolyzable ATP induces a compact conformation, where the lid segments of each subunit form a beta-stranded iris that closes over the central cavity of the complex. The structure of this closed state is also virtually the same in eukaryotic and archaeal chaperonins (Booth et al., 2008; Cong et al., 2010; Ditzel et al., 1998; Pereira et al., 2010; Zhang et al., 2010). The presence of an intact lid is dispensable for substrate binding and ATP hydrolysis in both eukaryotic and archaeal chaperonins. However, the lid confers allosteric coupling of subunits within the complex and is essential for substrate folding (Kanzaki et al., 2008; Meyer et al., 2003; Reissmann et al., 2007). Although the fully open and fully closed states are emerging in some structural detail, little is known about the trajectory of the chaperonin through the conformation cycle or how substrate folding is achieved (Bigotti and Clarke, 2008).

A number of studies using archaeal and eukaryotic chaperonins have suggested that ATP binding suffices to close the built-in lid and trigger substrate folding (Iizuka et al., 2003; Llorca et al., 2001; Villebeck et al., 2007; Stuart et al., 2011). Subsequent ATP hydrolysis would serve to reopen the lid and release the folded protein. In contrast, other studies reported that ATP binding alone is unable to close the lid or promote substrate folding (Bigotti et al., 2006; Meyer et al., 2003; Reissmann et al., 2007). Instead, these studies identified the transition state of ATP hydrolysis as the critical step in the ATPase cycle that promotes the closed conformation (Meyer et al., 2003; Reissmann et al., 2007).

A fundamental question for group II chaperonins concerns the fate of the substrate during the ATPase cycle. The current model proposes that group II chaperonins do not release the substrate during folding (Gómez-Puertas et al., 2004; Stuart et al., 2011). Instead, ATP binding would cause the apical domains with their bound substrate to move, and this movement mechanically forces substrate folding. In this view, substrate liberation occurs after nucleotide hydrolysis, perhaps after nucleotide release and the subsequent return of the chaperonin to the open state.

Some experimental results are not reconciled easily with the "mechanical force" model. The substrate-binding sites of group II chaperonins have been mapped to the vicinity of helix 11 (Spiess et al., 2006), which is unavailable to the central cavity in the ATP-induced closed state. The mechanical model of group II chaperonin action suggests that the cavity is not necessarily a folding chamber per se, rather it is used as a mechanical scaffold for active remodeling. This led to the suggestion that the lids primarily assist in the conformational cycle of the chaperonin (Kanzaki et al., 2008). However, ATP incubation of a group II chaperonin lacking a lid (Cpn-Δlid) produces an identical conformation to that of wild-type but is unable to promote substrate folding (Reissmann et al., 2007; Zhang et al., 2010). Thus, the movement of the apical domains does not require the presence of the lid; however, their movement alone is insufficient to promote folding.

Here, we use the group II chaperonin from mesophilic archaea *Methanococcus maripaludis*, herein Cpn, to define the fate of the polypeptide substrate during the conformational cycle of group II chaperonins. The allosteric regulation and structure of this Cpn are similar to those of TRiC/CCT (Pereira et al., 2010; Reissmann et al., 2007; Zhang et al., 2010). We find that ATP hydrolysis has a dual role in group II chaperonin function, promoting both lid closure and release of the substrate into the cavity. Importantly, both events must occur for successful substrate folding. We suggest an alternate model for group II chaperonin function, whereby folding relies on the release of the substrate into a unique chemical environment within the closed chamber.

RESULTS

A Single Round of Encapsulation within the Closed Chamber Suffices for Substrate Folding

We initially examined whether the folding reaction is completed within the closed central chamber of group II chaperonins. In principle, folding of a polypeptide with a strict chaperonin requirement, i.e., a stringent substrate, could require several cycles of Cpn binding and release (Figure 1A). Alternatively, the substrate could fold in a single ATPase-cycle event, without requiring multiple rounds of binding and release. To test these possibilities we employed rhodanese, a stringent Cpn substrate (Martin et al., 1991). ^{35}S-rhodanese binds to nucleotide-free Cpn in an unstructured, proteinase K (herein PK)-sensitive state (Figure 1A, left arrow, Figure 1B, lane 2 bottom panel, and Figure 1C for native gel analysis). Addition of ATP induces lid closure and encapsulates the substrate within the closed chamber (Meyer et al., 2003; Reissmann et al., 2007) (Figure 1A). Upon closure, the Cpn lid segments and the encapsulated ^{35}S-rhodanese are protected from proteolytic digestion (Figure 1B, lane 3). Importantly, ATP addition causes the time-dependent folding of rhodanese (Figure 1D, red symbols). Comparing the kinetics of rhodanese folding ($t_{1/2}$ ~12 min) with the estimated kinetics of a single round of ATP hydrolysis (Bigotti et al., 2006; Reissmann et al., 2007) indicates that completion of rhodanese folding involves several cycles of ATP binding and release. Similar results are observed for malate dehydrogenase (MDH) (see Figure S1B available online; data not shown). Importantly, addition of protease at any time following ATP addition interrupted the folding reaction (Figure 1D, PK, shown for t = 0 and t = 13 min). Because PK can only degrade the substrate if the lid is open, this result suggests that the Cpn-substrate complex undergoes repeated cycles of ATP-driven opening and closing during the folding reaction.

We next examined whether such iterative cycling is required to achieve folding by exploiting the observation that addition of AlFx together with ATP locks group II chaperonins in a symmetrically closed state that fully encapsulates the substrate (Meyer et al., 2003) (Figure 1A, right arrow). The ATP•AlFx-induced state of Cpn-rhodanese was locked closed, leading to full proteolytic protection of both Cpn and substrate (Figure 1B, lane 4) and a characteristic electrophoretic migration shift on native gels (Figure 1C). Under these conditions, ATPase cycling is interrupted (Figure S1A), and the substrate undergoes a single round of binding and encapsulation, allowing us to evaluate whether iterative cycling is required for group II chaperonin folding (Figure 1E). Strikingly, the rate and yield of rhodanese folding under these noncycling conditions were identical to those observed for the actively cycling chaperonin (Figure 1E). Addition of PK to the ATP•AlFx reaction did not interrupt folding, confirming that there was no reopening of the Cpn and no release of the nonnative substrate under these conditions. We conclude that the closed chamber of group II chaperonins is the folding-active compartment. Furthermore, a single round of encapsulation in this chamber can achieve maximum rhodanese folding, with similar kinetics and yield as observed under cycling conditions. Thus, although iterative cycling does occur, it is not strictly required for Cpn-dependent folding.

The Closed, Folding-Active, State of Group II Chaperonins Requires ATP Hydrolysis

To examine whether ATP binding suffices to promote the folding-active state of group II chaperonins, we specifically impaired the ATPase-active site by targeting Asp386, which is essential to

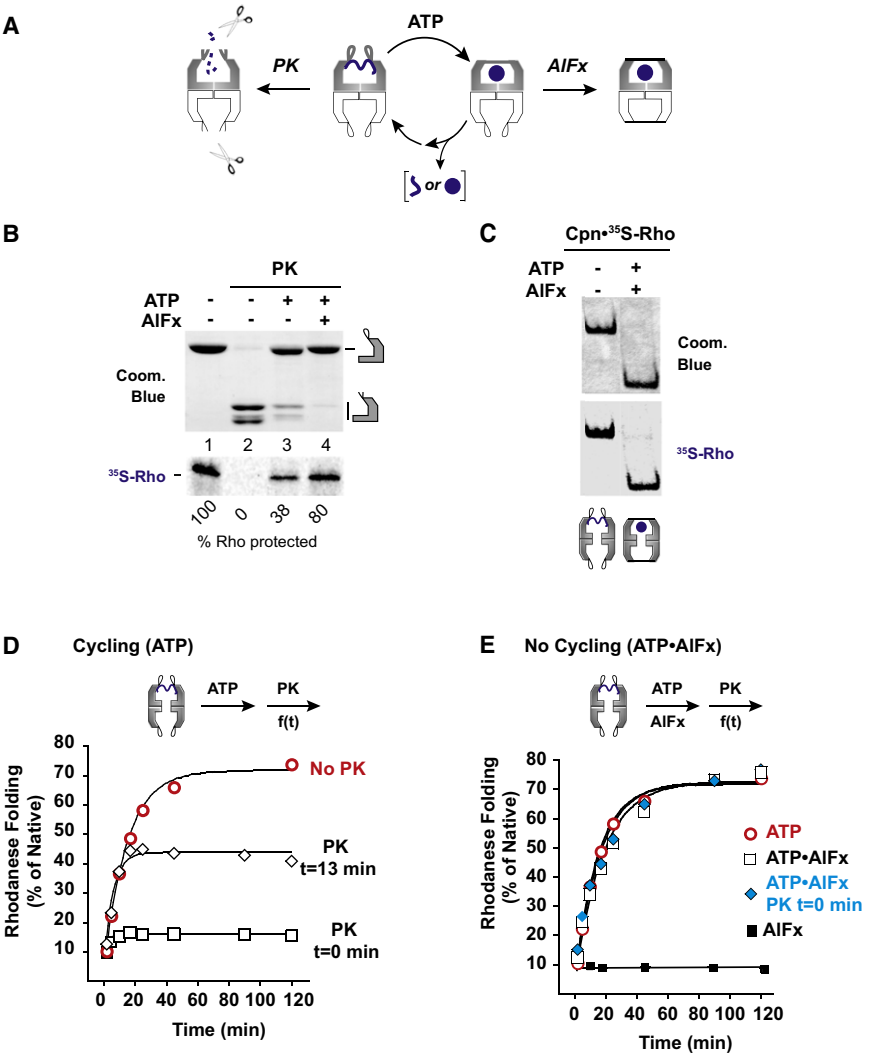

Figure 1. Role of Substrate Encapsulation and Iterative Cycling in Group II Chaperonin Action

(A) Cpn cycle between an open, substrate-accepting state, and an ATP-induced closed state. In each cycle the substrate (in blue) is released in either the folded or unfolded state. Unfolded substrate rebinds Cpn for iterative rounds of folding. Incubation with ATP and AlFx interrupts iterative cycling by locking Cpn in a closed state that encapsulates the substrate. In the absence of ATP, PK (scissors) digestion interrupts iterative cycling by specifically digesting the substrate (B) and the open lid segments in Cpn. (B) PK sensitivity of open and closed Cpn states. PK leads to full digestion of the open Cpn lids (Coomassie stain, top panel) and the bound substrate, ^{35}S-rhodanese (^{35}S-Rho, bottom panel; lane 2). ATP-induced cycling to the closed state protects both the Cpn lids and the substrate (lane 3). Incubation with ATP●AlFx locks the complex closed leading to complete PK protection of both lids and encapsulated ^{35}S-rhodanese (lane 4). A purified complex of Cpn●rhodanese at 0.25 μM was incubated in the presence or absence of 1 mM ATP and/or 1 mM AlFx for 10 min at 37°C and digested with 20 μg/ml PK for 5 min at 25°C. (C) Native gel analysis of Cpn-substrate complexes. Incubation with ATP●AlFx shifts the mobility of Cpn (top panel Coomassie blue stain), which carries the encapsulated substrate (bottom panel for autoradiography of ^{35}S-rhodanese). Nonnative rhodanese aggregates cannot migrate into the native gel (data not shown). (D) Folding under cycling conditions. ATP (5 mM) was added to initiate Cpn-mediated folding of rhodanese, measured at the indicated time points. Addition of PK at the times indicated immediately interrupts the folding reaction, indicating that the Cpn is cycling between open and closed states during folding. (E) Folding under noncycling conditions. Cpn mediated folding as in (D), except that folding was initiated either by addition of ATP (cycling allowed), ATP●AlFx (no cycling allowed), AlFx (control), or ATP●AlFx and PK (no cycling allowed, no rebinding of released Rho). The folding yields and rates were identical for all conditions, indicating that cycling is not required for group II chaperonin-mediated folding. See also Figure S1.

coordinate the water molecule that participates as a nucleophile during the hydrolysis of the phosphate-anhydride bond (Cpn-D386A) (Figure 2A). Cpn-D386A cannot hydrolyze ATP but retains efficient ATP binding (data not shown; Reissmann et al. [2007]). Importantly, unlike Cpn-WT, Cpn-D386A is unable to fold the stringent Cpn substrates rhodanese (Figure 2B) and malate dehydrogenase (data not shown). This demonstrates that ATP binding is insufficient to induce the fully folding-active state observed upon ATP hydrolysis.

We next assessed the proposal that ATP binding leads to partial (Clare et al., 2008) or full (Iizuka et al., 2003; Llorca et al., 2001) lid closure. To this end the structure of ATP-bound Cpn-D386A was derived to 15 Å resolution by single-particle cryo-EM (Figure 2C, blue). Comparison of these structures with the ATP-free and ATP-bound states of Cpn-WT, derived to 10 and 6 Å, respectively, revealed the conformational changes induced by ATP binding, distinguishing them from those induced by ATP hydrolysis (Figures 2D; Figure S2). ATP incubation with Cpn-WT induces lid closure, yielding a symmetrically closed structure similar to that previously obtained for Cpn-WT with ATP●AlFx (Figure 2C, cyan; see also Figure S5) (Pereira et al., 2010; Zhang et al., 2010). In contrast, ATP binding to Cpn-D386A yielded an open structure that resembled the nucleotide-free state (Figure 2D for overlay,; Figures S2A and S2B). Further addition of AlFx did not result in closure (data not shown). Despite leaving the lid open, ATP binding induced a ~20 Å constriction in the chaperonin opening (Figures 2D; Figure S2B, 110 Å span versus 130 Å in the ATP-free state). Closer analysis of the conformational changes in a single subunit indicated that ATP binding induces an en masse rigid body tilt of the entire intermediate and apical domains toward the ATP-binding equatorial domain (Figure S2C). We conclude that ATP binding is insufficient to close the lid but triggers domain movements that lead, upon hydrolysis, to the closed state. These results are

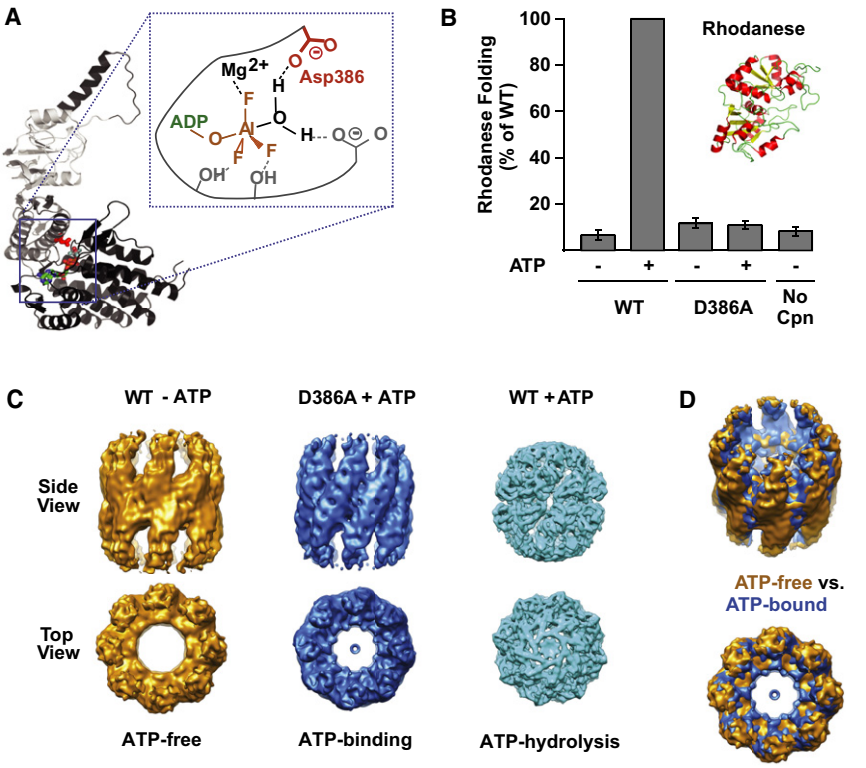

Figure 2. ATP Hydrolysis Is Required for the Closed Folding-Active State

(A) ATP-binding pocket of group II Cpn from *T. acidophilum* (pdb ID 1A6E) highlighting Asp386, essential for ATP hydrolysis.

(B) Rhodanese folding for Cpn-WT and Cpn-D386A. ATP hydrolysis is required to support rhodanese folding; data are represented as mean ± SEM (n = 3).

(C) Single-particle cryo-EM reconstructions of Cpn-WT and Cpn-D386A. Shown are side and top views of Cpn-WT without (left, gold) and with ATP (right, cyan) and Cpn-D386A with ATP (middle, blue).

(D) Overlay of EM density maps for Cpn-WT −ATP and Cpn-D386A +ATP highlights the changes induced by ATP binding.

(E) Role of ATP and ATP•AlFx on the ^{35}S-rhodanese interaction with Cpn-WT and Cpn-D386A. Cpn complexes were analyzed on 4% native gels, and the Rho-containing Cpn was visualized by autoradiography.

(F) PK digestion of Cpn-WT and Cpn-D386A complexes with ^{35}S-rhodanese, analyzed by SDS-PAGE followed by Coomassie blue staining (top), and autoradiography (bottom). Cpn-D386A is incapable of closing (compare lane 3 for WT with lane 6, lane 7 for D386A).

See also Figure S2.

consistent with fluorescence experiments on the thermosome from *Thermoplasma acidophilum*, indicating a rapid rearrangement attributed to ATP binding, followed by a slower rearrangement attributed to ATP hydrolysis and lid closure (Bigotti and Clarke, 2005; Reissmann et al., 2007).

The effects of ATP binding on the conformation of both the substrate and the lid were further examined using biochemical assays (Figures 2E and 2F). As described above, addition of ATP•AlFx to Cpn-WT stabilizes the closed state, locking the encapsulated substrate inside the chamber and leading to proteolytic protection of both the lids and the substrate (Figures 1B and 1C and Figures 2E and 2F, lane 3; top panel for Cpn, bottom panel for ^{35}S-Rho for ^{35}S-Rho-Cpn-WT complex). Both ATP and ATP•AlFx induce a structurally similar closed state in Cpn-WT (e.g., Figure 2C, right panel), but the ATP•AlFx state displays a characteristic faster electrophoretic migration on native gels (Figure 2E) (a similar effect is observed for TRiC/CCT [Meyer et al., 2003]). In contrast to Cpn-WT, incubation of Cpn-D386A with either ATP or ATP•AlFx failed to produce the signature mobility shift (Figure 2E). Furthermore, both the lid and the substrate remained in a largely unstructured, protease-sensitive state upon ATP binding (Figure 2F, lanes 5–7), consistent with the result that ATP binding leaves Cpn in an open state (Figures 2C and 2D). Importantly, the lid also remains open under conditions where only one ring binds nucleotide (0.2 mM; Reissmann et al. [2007]) or if Cpn-WT is incubated with the nonhydrolyzable ATP analogs AMPPNP or ATPγS (at either 0.2 or 1 mM; data not shown), further supporting the conclusion that ATP binding to either one ring or both does not suffice to close the lid.

ATP Hydrolysis Triggers Substrate Release from the Chaperonin-Binding Site

Lid closure and substrate encapsulation are essential for folding substrates such as actin for TRiC (Meyer et al., 2003) and rhodanese (Reissmann et al., 2007) and MDH for Cpn (Figures S3A and S3B). We next examined whether lid closure modulates the interaction of the substrate with the chamber. The "mechanical force" model proposes that the chaperonin does not release the substrate proteins into the closed cavity; in this scenario the chaperonin-substrate interaction persists in the closed state leading to the mechanical remodeling of the substrate

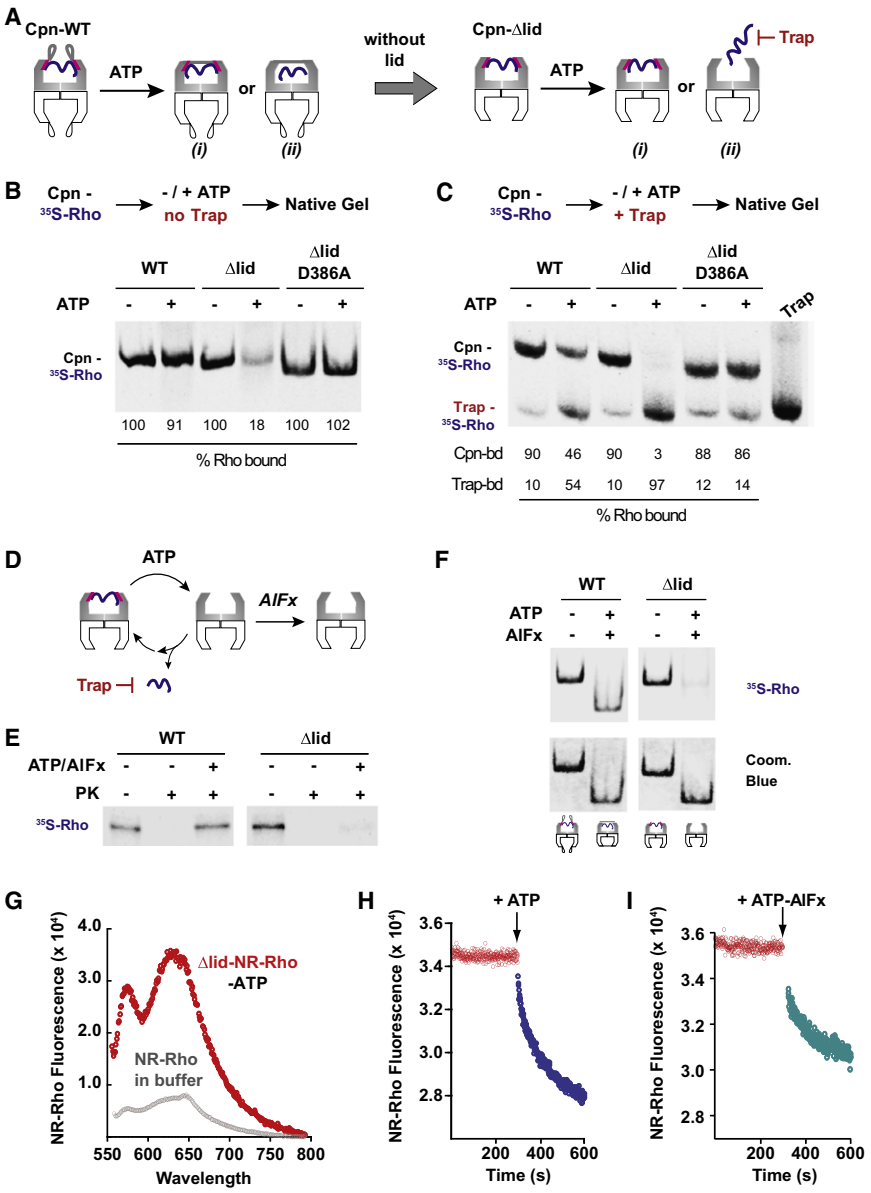

Figure 3. ATP Hydrolysis Triggers Substrate Release from Group II Chaperonins

(A) Proposed models for how closure affects substrate interactions with the central Cpn chamber. (i) The substrate remains bound in the closed state, or (ii) the substrate is released into the central cavity. The closed Cpn-WT retains substrate in either model (left). Removal of the lid, yielding Cpn-Δlid, allows testing of these models. Cpn-Δlid will lose the substrate if closure weakens the interaction with the chaperonin (model (ii) right). A decrease in substrate affinity might also be revealed using a GroEL-derived trap (Frydman and Hartl, 1996). Cpn substrate-binding sites shown as pink lines.

(B) Effect of ATP binding and hydrolysis on the Cpn-Δlid-substrate interaction. The indicated Cpn-^{35}S-rhodanese complexes, incubated with or without 1 mM ATP for 10 min at 37°C, were analyzed by native gel electrophoresis followed by autoradiography. The amount of ^{35}S-rhodanese that remains Cpn bound in each condition is indicated.

(C) Effect of ATP binding and hydrolysis on release of nonnative substrate from Cpn complexes. Autoradiography of native gel for reactions carried out as in (B), but in the presence of equimolar GroEL-Trap, which functions as a scavenger for released nonnative proteins. A reaction where denatured rhodanese is added directly to the Trap is included as a control. The amount of Cpn-bound and Trap-bound rhodanese was calculated for each reaction from the native gel analysis.

(D) Transition state mimic ATP●AlFx locks the Cpn-Δlid in the symmetrically closed state immediately halting the ATPase cycle (see Figure S1; Zhang et al. [2010]).

(E) PK digestion of ^{35}S-rhodanese complexes with Cpn-WT or Cpn-Δlid in the presence or absence of ATP●AlFx. The ^{35}S-rhodanese is completely digested in the closed Cpn-Δlid.

(F) Native gel analysis of ^{35}S-rhodanese-chaperonin complexes incubated as in (E). Cpn-Δlid + ATP●AlFx fully releases its substrate (top panel, ^{35}S-Rho) even though both Cpns undergo the same conformational change with ATP●AlFx (bottom panel; Coom. Blue).

(G) Fluorescence emission spectra of NR-Rho in the presence and absence of Cpn-Δlid (Kim et al., 2005). Binding to the Cpn causes an increase in fluorescence intensity at 630 nm.

(H) Time-dependent changes in the fluorescence intensity of NR-Rho emission at 630 nm. Red trace indicates NR-Rho-Cpn-Δlid complex in the absence of ATP. Addition of ATP (arrow) causes a decrease in fluorescence (blue trace).

(I) Time-dependent changes in the fluorescence intensity of NR-Rho emission at 630 nm as in (H); arrow indicates addition of ATP●AlFx, which causes a qualitatively similar decrease in fluorescence intensity (cyan trace).

See also Figure S3.

conformation (Figure 3Ai, left) (Llorca et al., 2001). Alternatively, ATP hydrolysis could promote substrate release into the closed chamber (Figure 3Aii, left). Because monitoring the substrate-chaperonin interaction inside the closed chamber is complicated by the presence of the lid, we exploited the previously characterized Cpn-Δlid variant that lacks the entire lid-forming segments (Pereira et al., 2010; Reissmann et al., 2007; Zhang et al., 2010). Importantly, Cpn-Δlid achieves the same ATP-induced "closed" conformation as Cpn-WT (Zhang et al., 2010), and its ATPase activity and substrate-binding ability are unaffected (Reissmann et al., 2007). These features of Cpn-Δlid allowed us to distinguish between the above models (Figure 3A, right panels). Thus, the model that proposes that the polypeptide remains associated with the chaperonin throughout the ATPase cycle predicts that the substrate will remain bound to Cpn-Δlid upon addition of ATP or ATP●AlFx (Figure 3Ai, "Δlid" right). In contrast if ATP weakens the chaperonin-substrate interaction, the absence of the lid will allow the polypeptide to diffuse

away from the chaperonin (Figure 3Aii, "Δlid" right). Of note, Cpn-Δlid cannot promote folding of substrates such as rhodanese and MDH (Figures S3A and S3B; Reissmann et al. [2007]); thus, substrate release from Cpn-Δlid cannot be ascribed to completion of folding.

Purified ^{35}S-rhodanese•Cpn complexes were incubated in the presence or absence of ATP for 10 min and analyzed using native gels followed by autoradiography (Figure 3B). Cpn-WT comigrates with the substrate under both conditions (Figure 3B, WT), as expected given that ^{35}S-rhodanese is encapsulated in the closed complex (Figures 1B and 1C). The small ATP-induced reduction in bound substrate is presumably due to loss through ATPase cycling and/or folding (see below, Figure 3C). Strikingly, incubation of Cpn-Δlid with ATP led to a dramatic reduction in the amount of Cpn-bound rhodanese (Figure 3B, Δlid). This ATP-dependent loss of rhodanese required ATP hydrolysis because it was not observed when the Cpn-Δlid also carried the D386A mutation (Figure 3B, Δlid/D386A). Similar results were obtained for other Cpn-bound polypeptides, including MDH (data not shown) and actin (see below; Figure 5).

The ATP-induced reduction in Cpn-substrate affinity was further evinced through the use of a "Trap," a modified GroEL that scavenges nonnative polypeptides (Figure 3C) (Frydman and Hartl, 1996). Trap will not bind to folded rhodanese but will bind to nonnative polypeptides once they are released from the Cpn (Frydman and Hartl, 1996) (Figure 3C, see Trap lane). For all Cpn variants tested, little or no ^{35}S-rhodanese was captured by the Trap in the absence of ATP, suggesting that rhodanese binds stably to all nucleotide-free Cpn variants and cannot be displaced by the Trap (Figure 3C, −ATP). Addition of ATP to Cpn-WT allowed a fraction of rhodanese to bind to the more rapidly migrating Trap (Figure 3C, WT+ATP). Comparing the WT incubations in the presence and absence of Trap (i.e., Figures 3B and 3C) suggests that during normal ATP cycling a fraction of the substrate is released in a nonnative form that rebinds to the chaperonin for another round of folding. This nonnative polypeptide is captured by the Trap, which thus prevents Cpn rebinding and interrupts the cycle. Importantly, addition of ATP to Cpn-Δlid-^{35}S-rhodanese caused a near-complete transfer of the bound polypeptide to the Trap (Figure 3C, Δlid), indicating that ATP induces substrate release from the chaperonin. Furthermore, no increase in substrate transfer to the Trap was observed upon ATP addition to Cpn-Δlid D386A (Figure 3C, Δlid/D386A), indicating that substrate dissociation from Cpn requires ATP hydrolysis.

The experiments above show that ATP hydrolysis has a function that is completely lid independent, namely, to release the substrate from the chaperonin-binding sites. We next employed ATP•AlFx, which mimics the trigonal-bipyramidal transition state of ATP hydrolysis (Meyer et al., 2003) (Figure 3D). As with Cpn-WT (Figure S1A), the addition of AlFx to Cpn-Δlid immediately arrests its ATPase activity, suggesting that inhibition of ATP hydrolysis and trapping of the closed state occurs after a single cycle (Figure S3C). Whereas incubation of Cpn-WT-^{35}S-rhodanese with ATP•AlFx closes the chamber and encapsulates the substrate (Figures 3E and 3F), the substrate remains protease sensitive following incubation of Cpn-Δlid-^{35}S-rhodanese with ATP•AlFx (Figure 3E). Native gel analysis showed that Cpn-Δlid with ATP•AlFx undergoes the same signature shift as Cpn-WT, consistent with structural analyses showing that both Cpns adopt the same closed conformation upon incubation with ATP•AlFx (Pereira et al., 2010; Zhang et al., 2010). ATP•AlFx induced a complete release of a broad panel of polypeptides (Figure 3F for ^{35}S-rhodanese; Figures S3D–S3G for other substrates; Figure 5 for Actin), indicating that ATP hydrolysis blocks general access to the substrate-binding sites. The same conclusion was reached using size exclusion chromatography of purified Cpn-^{35}S-rhodanese complexes incubated in the presence or absence of ATP•AlFx and analyzed on a Bio-Sil SEC-400-5 column (Figure S3H). This experiment also indicated that ATP•AlFx induces full substrate release from Cpn-Δlid.

The effect of nucleotide hydrolysis on Cpn-substrate interactions was further examined using rhodanese carrying the environmentally sensitive fluorescent moiety Nile Red (Kim et al., 2005) (herein NR-Rho; Figures 3G–3I). In free solution, NR-Rho exhibits a low fluorescence emission spectrum characteristic of an aqueous, polar environment, with a maximum at ~650 nm (Figure 3G, gray trace). However, binding to Cpn caused a fluorescence intensity increase as well as a blue shift of the maximal intensity to ~630 nm (Figure 3G, red trace for Cpn-Δlid; similar results obtained for Cpn-WT; data not shown). This change in fluorescence upon Cpn binding is a diagnostic for rhodanese occupying a more hydrophobic environment (Kim et al., 2005). We used the maximal fluorescence at 630 nm to monitor the effect of nucleotides on the substrate-chaperonin interaction. The Cpn-Δlid-NR-Rho fluorescence signal remained stable in the absence of nucleotide (Figures 3H and 3I, red traces). Addition of ATP produced a rapid decay in fluorescence intensity (Figure 3H, "+ATP," blue trace). This supports our previous conclusion that ATP cycling by Cpn leads to substrate release. Addition of ATP•AlFx yielded similar results (Figure 3I, "+ATP•AlFx," cyan trace), supporting the idea that the ATP hydrolysis-transition state induces substrate release. We conclude that ATP hydrolysis has a dual function within the chaperonin cycle; it promotes lid closure (Figure 2) and also triggers substrate release from the chaperonin-binding sites (Figure 3). Strikingly, the latter function is not dependent on the presence of a lid.

The Chaperonin Substrate-Binding Sites Are Unavailable in the Closed State

A simple model explaining our results is that the ATP-induced Cpn conformation no longer exposes the substrate-binding sites. We tested this model using an order of addition experiment (Figure 4). In the control condition (Figure 4, Ctrl), substrate was added to the open, apo-Cpn, which exposes the substrate-binding sites. The second condition added the substrate first, prior to incubation with ATP•AlFx (Figure 4, S→A); this condition measured the extent of ATP•AlFx-induced substrate release. In the third condition we incubated with ATP•AlFx first and then added substrate to the chaperonin (Figure 4, A→S); this measured the ability of an ATP•AlFx-preincubated closed complex to bind substrate (Figure 4A). If the binding sites are still available in the closed state, we might expect some substrate binding for closed Cpn-Δlid in the A→S condition, which still retains a large opening allowing access to the central cavity (Pereira et al., 2010; Zhang et al., 2010). Because the pore size may restrict polypeptide entry to

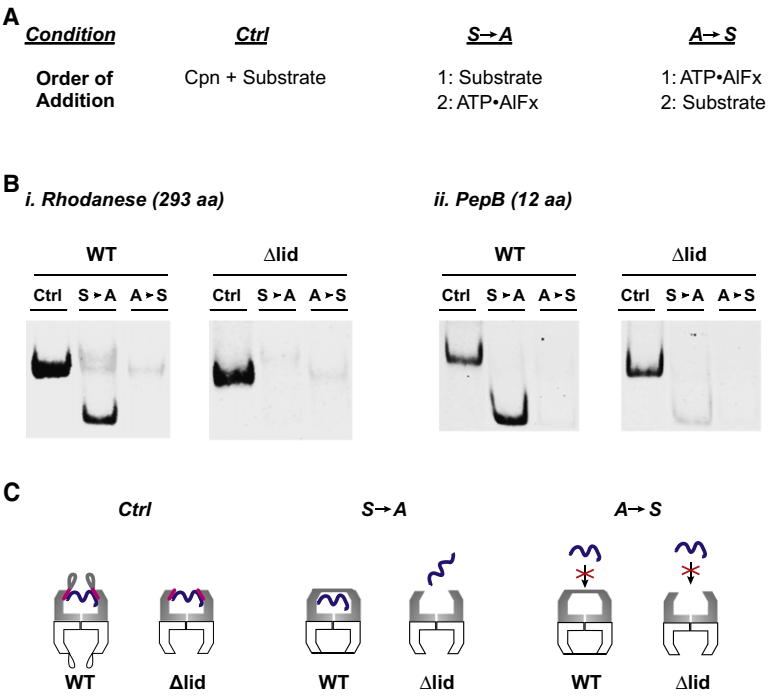

Figure 4. The Substrate-Binding Sites Are Unavailable in the Closed Cpn State

(A) Order of addition experiment to test availability of substrate-binding sites in the open and closed Cpn states. Without nucleotide, both Cpn-WT and Cpn-Δlid are open and bind substrate (Ctrl). Substrate addition prior to incubation with ATP●AlFx allows the substrate to bind first before closure (S→A); incubation with ATP●AlFx prior to substrate to addition examines if the closed state can bind substrate (A→S).

(B) Native gel analysis of the above incubations. Two Cpn-binding substrates of different sizes were used: (i) rhodanese (293 aa), and (ii) PepB (12 aa). The smaller peptide should access more readily the substrate-binding sites. ^{35}S-Rhodanese was detected by autoradiography; Alexa 488-PepB was detected by fluorescence scan.

(C) With Ctrl, both substrates bind chaperonin in the open state. S→A shows that when the lid is present (Cpn-WT), closure of the Cpn-substrate complex retains the substrate in the chamber; when the lid is absent (Cpn-Δlid), the substrate escapes the cavity. A→S illustrates how the ATP●AlFx state blocks substrate binding to both Cpn-WT and Cpn-Δlid. Because Cpn-Δlid retains access to the inner chamber in the closed state, this result indicates that the substrate-binding sites are hidden in the closed state.

the cavity and may sterically interfere with substrate binding, we used both rhodanese (Figure 4Bi) and a small 12-mer peptide substrate (herein PepB) (Figures S3G; Figure 4Bii). The small peptide substrate should be able to freely diffuse inside the closed chamber in the Cpn-Δlid.

In the absence of nucleotide, both substrates bound to Cpn-WT and Cpn-Δlid (Ctrl; Figures 4B and 4C; Figure S3G). As expected, addition of ATP●AlFx to the Cpn-substrate complex (Figure 4, S→A) promoted substrate encapsulation for Cpn-WT (WT S→A) (Figures 4B and 4C) and substrate release for Cpn-Δlid (Δlid S→A) (Figures 4B and 4C). In the case of A→S, closing the Cpn-WT chamber with ATP●AlFx precluded substrate binding; thus, the closed lid blocks access to the central cavity (WT A→S) (Figure 4B and scheme in Figure 4C). For Cpn-Δlid, substrate should bind the chaperonin in the A→S condition provided that the binding sites are still available in the closed conformation. This was not the case; instead the ATP●AlFx preincubated Cpn-Δlid was unable to bind either ^{35}S-rhodanese or the small PepB (Figure 4B) (Cpn-Δlid compare S→A and A→S). Thus, the ATP●AlFx state of Cpn-Δlid no longer exposes the substrate-binding sites. Given that the ATP●AlFx conformations of Cpn-WT and Cpn-Δlid are virtually identical (Pereira et al., 2010; Zhang et al., 2010), these experiments show that the substrate-binding sites are no longer available upon ATP hydrolysis.

Mechanism of ATP-Induced Substrate Release

What is the possible mechanism for substrate release in group II chaperonins? A structural analogy with the distantly related bacterial group I chaperonins, e.g., GroEL, is not possible, given that they use a detachable lid, GroES, which upon ATP binding, both caps the cavity and displaces the substrate. In contrast we show that substrate release in group II chaperonins is lid independent and requires ATP hydrolysis.

Closer examination of Cpn structures in the open and closed states led to a hypothesis for how ATP hydrolysis induces substrate eviction (Figure 5A) (Pereira et al., 2010; Zhang et al., 2010). In the open state the substrate-binding region around helix 11 is well exposed (Figure 5A, pink in left panel) (Spiess et al., 2006), leaving ample space to accommodate the bound substrate. In contrast the closed state brings the apical domains from adjacent subunits into close proximity (Figure 5A). Closure causes helix 11 to form a tightly packed interface with a loop spanning residues 327–331 in its neighboring subunit (Figure 5A, cyan). Such lateral intra-ring contacts might displace the substrate from its binding site, causing the 327–331 region to act as a "*r*elease *l*oop for the *s*ubstrate" (herein *rls* loop). To disrupt this lateral interface, we made Ala substitutions in four loop residues making key contacts with helix 11 yielding the Cpn-rls variants (Figure 5A, T327A, N328A, K330A, and D331A). To better understand the role of the *rls* loop within the chaperonin cycle, we used cryo-EM to obtain a detailed structural characterization of the conformation of both Cpn-rls and Cpn-rls-Δlid in the presence or absence of ATP or ATP●AlFx (Figure S4A for Fourier shell correlation analysis of resolutions; Figure S4B for Cpn-rls-Δlid; and Figure S5 for Cpn-rls). The *rls* chaperonins achieve essentially the same closed state as the wild-type counterparts (Figures 5B and 5C; Figure S4B for Cpn-rls-Δlid; Figure S5 for Cpn-rls). Consistent with their ability to reach a closed state, the Cpn-rls mutants were competent for ATP binding and hydrolysis (data not shown).

We initially focused on Cpn-rls-Δlid because the absence of a lid simplifies analysis of substrate release (Figures 5D–5F).

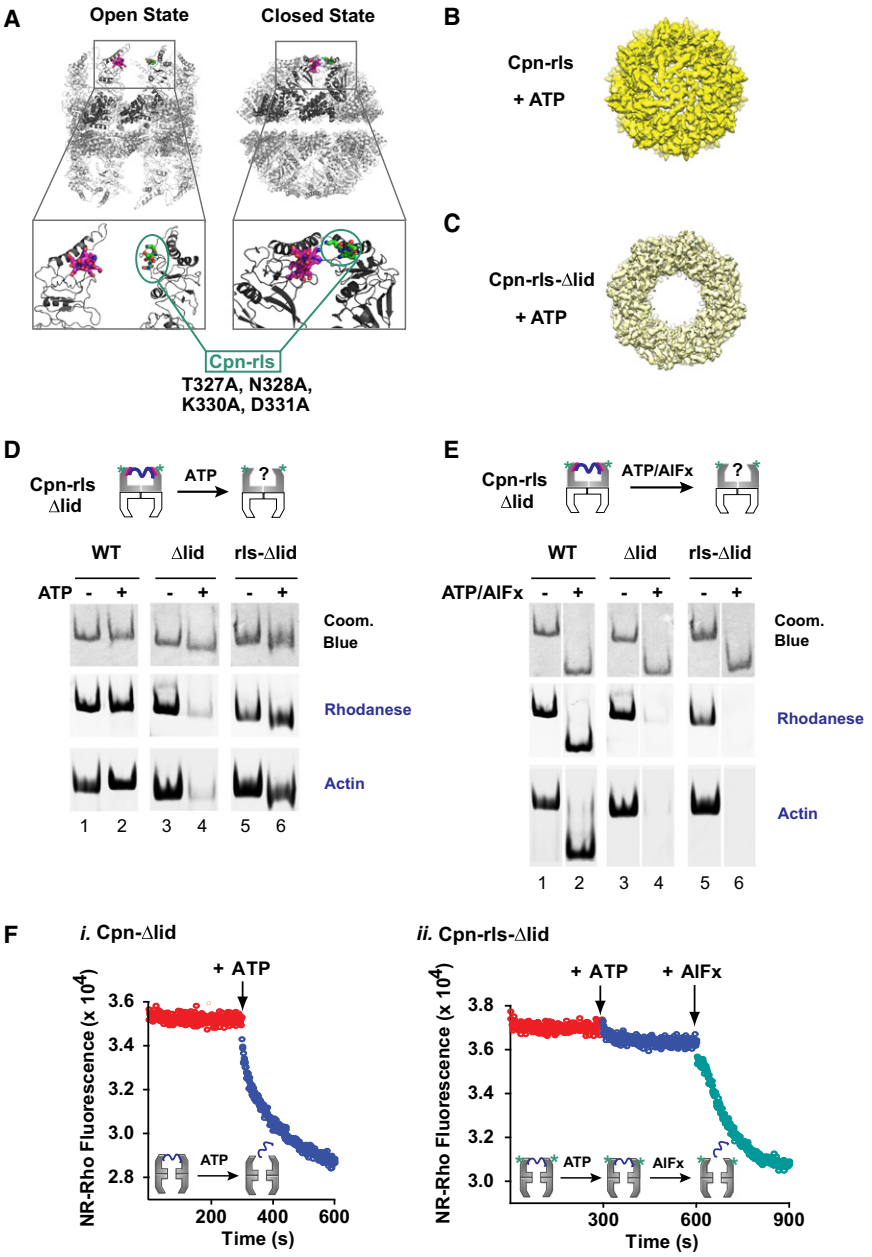

Figure 5. Structural Basis of ATP-Induced Substrate Release in Group II Chaperonins

(A) Structures of group II chaperonins in the open and closed states highlighting helix 11, the locus of substrate binding (pink). ATP-induced closure brings together adjacent apical domains, creating a tight interface between helix 11 of one subunit and loop 327–331 of the neighboring subunit (green). The indicated tetra-alanine substitution in loop 327–331 (herein *rls*) was introduced in both Cpn and Cpn-Δlid (herein Cpn-rls and Cpn-rls-Δlid).

(B and C) ATP induces the compact closed state in Cpn-rls (B) and Cpn-rls-Δlid (C). Top view of structures of indicated Cpn states obtained by single-particle cryo-EM reconstructions to 4–6 Å (see also Figure 6, Figure S4, and Figure S5).

(D) ATP fails to induce substrate release in Cpn-rls-Δlid. The indicated Cpn-substrate complexes were incubated in the presence and absence of ATP; substrate release assessed using native gel electrophoresis followed by Coomassie staining to visualize the Cpn(s) (top panel) and fluorescence scans to view substrate(s) (middle and bottom panels).

(E) ATP●AlFx triggers substrate release in Cpn-rls-Δlid. Incubations and analysis as in (D), except that incubations were carried out in the presence and absence of ATP●AlFx.

(F) Nucleotide-induced changes in the environment of NR-Rho bound to Cpn-Δlid (i) or Cpn-rls-Δlid (ii). Experiments performed as in Figure 3H. Starting from a nucleotide-free NR-Rho-Cpn complex (red trace), ATP was added to reaction at time indicated by an arrow (blue trace) and incubation continued. For Cpn-rls-Δlid no drop in fluorescence was observed upon ATP addition; after 5 min, AlFx was added to the ATP reaction and incubation continued (cyan trace).

See also Figure S4.

Cpn-WT and Cpn-Δlid served as controls. In the absence of ATP, all chaperonins bound rhodanese and actin efficiently, as shown by native gel analysis (Figure 5D). Strikingly, Cpn-rls-Δlid was incapable of releasing either substrate in the presence of ATP, unlike Cpn-Δlid (Figure 5D, compare lane 6 to lane 4). This suggests that the lateral contacts between helix 11 and the *rls* loop 327–331 are indeed important for releasing the substrate upon ATP hydrolysis.

We next examined the effect of the transition state mimic ATP●AlFx (Figure 5E). Native gel analysis showed that Cpn-rls-Δlid adopts the same fast migrating conformation observed for Cpn-Δlid and Cpn-WT (Figure 5E, Coomassie blue panel), consistent with the cryo-EM analysis. Surprisingly, unlike ATP, incubation with ATP●AlFx caused Cpn-rls-Δlid to efficiently release all the substrates tested (Figure 5E for rhodanese and actin). This observation was striking given the apparent similarity between the ATP and ATP●AlFx structures of Cpn-rls variants (Figure 5E; Figure S4B). Thus, it appears that, in the *rls* mutant, the conformation promoting substrate release cannot be stably populated by ATP alone, whereas ATP●AlFx can stabilize this state and evict the substrate.

Fluorescence spectroscopy provided independent support for the above conclusions. As for Cpn-Δlid, NR-Rho bound to Cpn-rls-Δlid had an emission spectrum characteristic of a hydrophobic environment (data not shown). In contrast to Cpn-Δlid (Figure 5Fi, blue trace), ATP incubation did not cause any appreciable change in the fluorescence of NR-Rho bound to Cpn-rls-Δlid (Figure 5Fii, blue trace), indicating that ATP alone cannot release the bound substrate. However, when AlFx was

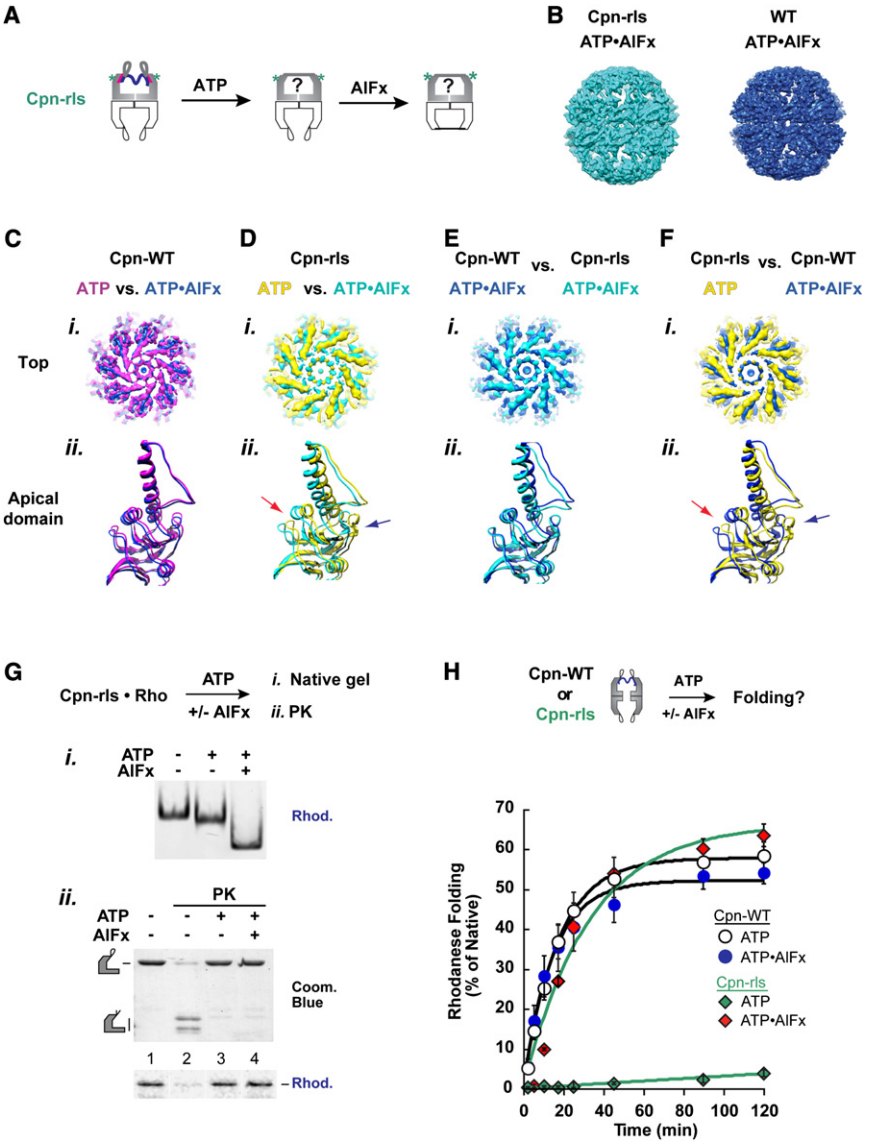

Figure 6. Substrate Release into the Central Chamber Is Required for Group II Chaperonin-Mediated Folding

(A) Use of Cpn-rls to test the role of substrate release in group II chaperonin folding. Incubation with ATP should lead to lid closure without substrate release, whereas addition of ATP●AlFx should release the substrate into the closed cavity.

(B) Side views of single-particle cryo-EM reconstructions of ATP●AlFx induced state of Cpn-rls and Cpn-WT highlight the similarity of both closed structures (see also below; Figure S5).

(C–F) Comparative structural analysis of the ATP and ATP●AlFx states of Cpn-WT and Cpn-rls. i. Top views of overlays for the electron density maps. ii. Superimposition of apical domain region for a single subunit from the overlaid chaperonin models. Superimposition of structures obtained for Cpn-rls and Cpn-WT reveals that the ATP state of Cpn-WT (purple) is virtually identical to the ATP●AlFx states of both Cpn-WT (blue) and Cpn-rls (cyan). In contrast, ATP induces a different closed state in Cpn-rls (yellow); comparison with ATP●AlFx states reveals major differences in the position of helix 11 (red arrow) and the *rls* loop (blue arrow, residues 327–331).

(G) Cpn-rls binds rhodanese efficiently and encapsulates the substrate upon ATP or ATP●AlFx induced closure. i. Native gel analysis of ^{35}S-rhodanese bound to Cpn-rls in the presence or absence of ATP or ATP●AlFx. ii. PK digestion of incubations from (i). Cpn-rls produces a protease-resistant lid in the presence of ATP or ATP●AlFx (top panel) that fully encapsulates the substrate (bottom panel for ^{35}S-rhodanese). Note similarity with Cpn-WT in Figures 2E and 2F.

(H) Rhodanese folding requires substrate release into the central chamber. Rhodanese complexes with Cpn-WT or Cpn-rls were incubated with the indicated nucleotides, and folding was assessed as in Figure 1; data are represented as mean ± SEM (n = 3).

See also Figure S5.

added to an ongoing incubation of NR-Rho●Cpn-rls-Δlid with ATP, the fluorescence rapidly dropped, indicating substrate release from the chaperonin (Figure 5Fii, cyan trace). A similar reduction in fluorescence intensity was observed if ATP and AlFx were added together but was absent if only AlFx was added (data not shown). We conclude that weakening the lateral contacts between helix 11 and its neighboring subunit prevents substrate release, even though Cpn-rls-Δlid can hydrolyze ATP and achieve the closed state. However, stabilizing the post-hydrolysis state by addition of AlFx populates the conformation that evicts the substrate.

Structural Basis of Substrate Release and Encapsulation

We next examined the effect of the *rls* mutations in the Cpn with the intact lid (herein Cpn-rls, Figure 6). Detailed structural analyses of the ATP and ATP●AlFx induced states in both Cpn-WT and Cpn-rls revealed interesting differences between these chaperonins (Figures 6B–6F; Figure S5). Single-particle cryo-EM reconstructions were obtained to 4–6 Å for both chaperonins in the presence of either ATP or ATP●AlFx (Cpn-WT-ATP 6 Å, Cpn-WT-ATP●AlFx 4.3 Å, Cpn-rls-ATP 5 Å, Cpn-rls-ATP●AlFx 6 Å, Figure 6; Figure S5). Models of these structures were then built by flexible fitting into the density map with Rosetta (Figure 6; Figure S5A; see Figure S5B for goodness of fit between model and density map) (DiMaio et al., 2009). Cpn-rls achieved a closed state with either ATP or ATP●AlFx, similar to those obtained with Cpn-WT. Notably, superimposition of the structures of Cpn-WT and Cpn-rls in the different nucleotide states revealed variations in their structure, particularly in the region corresponding to the apical domains (Figures 6C–6F; i. top view of superimposed EM density

maps). These differences were also evident when comparing the apical domain regions in the respective chaperonin models (Figures 6C–6F; ii. detail of apical domain and lid for a subunit within the complex). The ATP (magenta) and ATP•AlFx (blue) states of Cpn-WT were essentially identical (Figure 6C). Thus, ATP•AlFx generates the same closed state observed under ATP-cycling conditions (e.g., Figure 1E). Importantly, we observed a shift in the apical domain regions between the closed Cpn-rls states induced by ATP (yellow) and ATP•AlFx (cyan) (Figure 6D). Cpn-rls-ATP also exhibited noticeable differences with both closed WT structures (e.g., Figure 6F). The apical domain protrusions in Cpn-rls-ATP are shifted clockwise, and the apical domains, including the lid, are tilted up compared to the ATP•AlFx state, exhibiting significant variations in helix 11 (ii. red arrow) and the *rls* loop (ii. blue arrow). In contrast the ATP•AlFx states of Cpn-WT and Cpn-rls were nearly identical (Figure 6E). These structural analyses demonstrate that even though Cpn-rls can close with ATP, impairment of the helix 11/loop 327–331 contacts results in aberrant intra-ring interactions between the apical domains. This is consistent with the inability of Cpn-rls-Δlid to release the substrate in the presence of ATP (Figure 5Fii). Furthermore, ATP•AlFx induces a closed conformation in Cpn-rls that is indistinguishable from the closed state of Cpn-WT with either ATP or ATP•AlFx. This is consistent with, and explains, the finding that ATP•AlFx leads to substrate release in Cpn-rls-Δlid (Figure 5Fii).

Substrate Release and Encapsulation Are Required for Productive Folding

The identification of a mechanism that evicts the bound polypeptide upon closure allowed us to test the relevance of substrate release for the folding cycle. First, the ability of Cpn-rls to encapsulate a bound substrate was examined by native gel analysis (Figure 6Gi) and PK digestion (Figure 6Gii), as shown above for Cpn-WT. Incubation of the Cpn-rls with rhodanese yielded a binary complex that behaved exactly as that of Cpn-WT (Figure 6Gi). Protease digestion analysis indicated that, in the absence of nucleotide, the substrate binds in an unstructured conformation (Figure 6Gii, lane 2). Importantly, incubation with either ATP or ATP•AlFx led to proteolytic protection of both the chaperonin lid segments (Figure 6Gii, lanes 3 and 4, top panel) and the bound ^{35}S-rhodanese (Figure 6Gii, lanes 3 and 4, bottom panel). Thus, both ATP and ATP•AlFx induce stable lid closure and fully encapsulate the substrate within the central chamber of Cpn-rls.

Rhodanese-chaperonin complexes were prepared for Cpn-rls and Cpn-WT, which served as a control (Figure 6H). As expected, addition of ATP or ATP•AlFx to the Cpn-WT complex induced rhodanese folding (Figure 6H, black traces). Strikingly, addition of ATP to the Cpn-rls complex failed to promote rhodanese folding, even though the substrate was encapsulated within the closed chamber (Figure 6H, green trace). We hypothesized that failure to fold stems from the failure to release the bound substrate into the central chamber. Therefore, we tested the effect of ATP•AlFx, which should promote substrate release (Figure 5). Addition of ATP•AlFx to the Cpn-rls reaction caused efficient rhodanese folding (Figure 6H). These experiments indicate that lid closure and substrate encapsulation are, by themselves, unable to promote substrate folding. Importantly, they demonstrate that substrate release into the central closed chamber is essential for productive folding by group II chaperonins.

DISCUSSION

Our study defines how the ATPase cycle of group II chaperonins modulates the interaction with substrates (Figure 7). We find that ATP hydrolysis triggers substrate release from the chaperonin through a hitherto unanticipated mechanism involving lateral intra-ring contacts between adjacent apical domains. Given the high degree of structural and mechanistic similarity among all group II chaperonins, our findings have broad implications to understand cellular folding in eukaryotes and archaea.

Role of ATP Binding in the Chaperonin-Conformational Cycle

To resolve the role of ATP binding in group II chaperonin action, we specifically impaired hydrolysis by targeting D386 (Ditzel et al., 1998). We find that ATP binding alone does not support substrate folding or lid closure, similar to previous findings for TRiC/CCT (Meyer et al., 2003). ATP binding does induce a conformational change that constricts the Cpn chamber entrance from 130 to 110 Å (Figure S2; Figures 7A and 7B). The movement results from an en bloc counterclockwise rotation of the intermediate and apical domains with respect to the equatorial, ATP-binding domain (Figure S2). Notably, a similar concerted movement of intermediate and apical domains has previously been observed during lid closure for TRiC/CCT (Booth et al., 2008). Our results indicate that ATP hydrolysis is generally required for lid closure and folding in group II chaperonins, underscoring the general conservation of architecture and mechanism between archaeal and eukaryotic chaperonins.

The Closed Group II Chaperonin Chamber Is a "Folding-Active" Compartment

ATP hydrolysis has a dual role within the group II chaperonin cycle: it both triggers lid closure and releases the substrate from the apical domains into the cavity (Figure 7). Importantly, both events are required for productive folding. Lid closure in the absence of substrate release is also insufficient to achieve folding (Figure 6H). This contrasts with the previously proposed mechanical force model, which suggests that folding occurs through movement of the apical domains without releasing the substrate. The observation that we can generate a chaperonin state that can close the lid without releasing the substrate raises the possibility that lid closure and substrate encapsulation precede release (Figures 7A and 7B, shown in brackets). Such a mechanism would ensure that substrates are confined inside the chamber prior to their release, thereby avoiding the premature escape of nonnative aggregation-prone species into the cytosol.

The released substrate folds while encapsulated in the central cavity (Figure 1E). No folding was observed when the substrate was released into the bulk solution (Cpn-Δlid) (Figures S3A and S3B), indicating that the chemical and physical characteristics of the closed central chamber create a folding-active compartment. The nature of this compartment will depend on the side

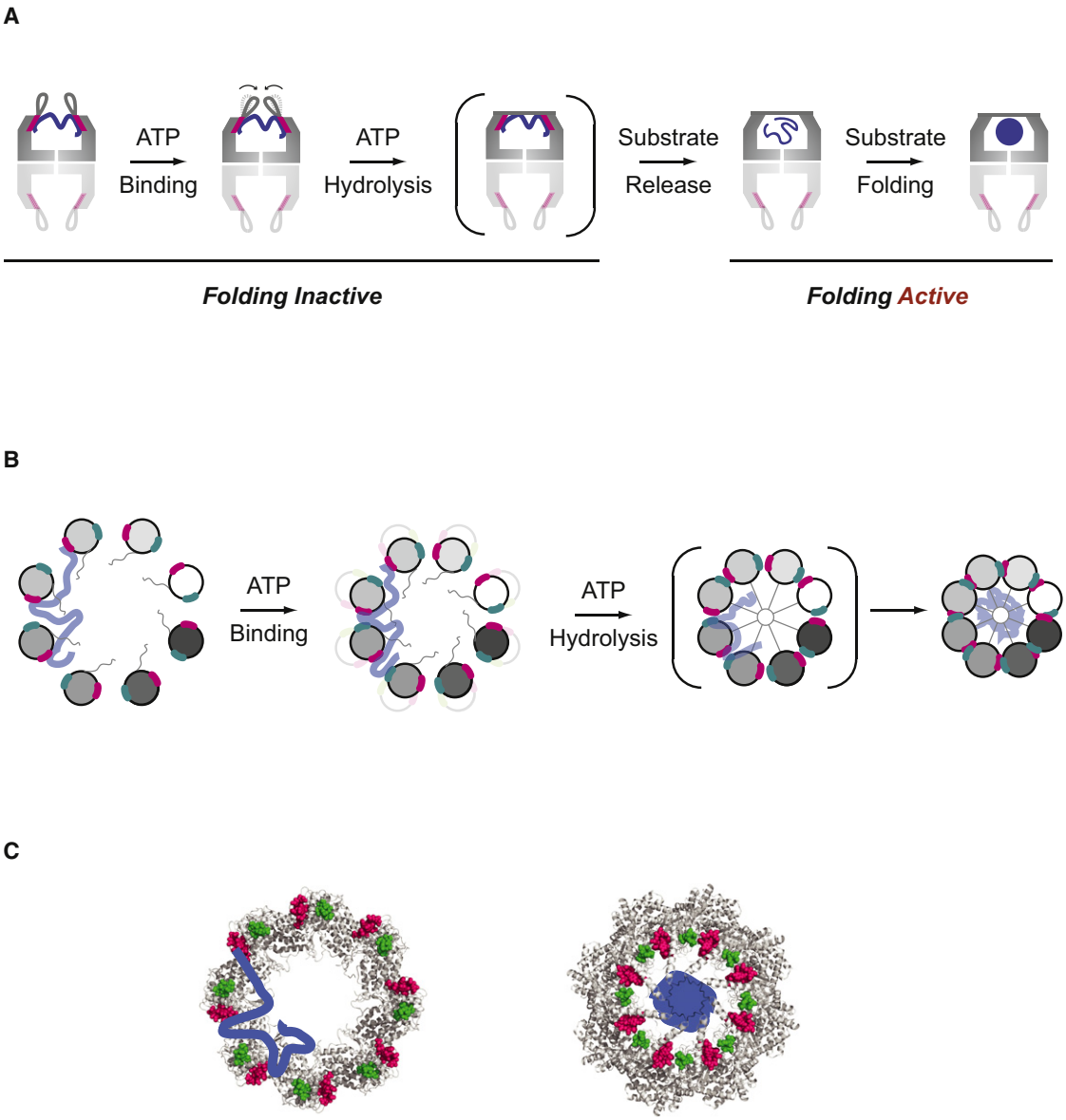

Figure 7. Model for Group II Chaperonin-Folding Mechanism

(A) ATP regulation of the Cpn substrate cycle. In the absence of ATP, chaperonins are open, exposing substrate-binding sites (pink). Upon ATP binding, the lid remains open and the substrate bound, but a subtle conformational change is observed. ATP hydrolysis has a dual function: close the lid, and release the substrate by hiding the substrate-binding sites. We hypothesize that lid closure may precede substrate release, transiently generating a closed but folding-inactive state (in brackets). Substrate release into the closed chamber is required for folding, which occurs within the central chamber.

(B) Top view of the chaperonin-substrate cycle in (A), highlighting the mechanism of polypeptide release upon ATP hydrolysis. The open, ATP-free and ATP-bound, states expose the substrate-binding region (pink). ATP hydrolysis creates a lateral contact with the *rls* loop (green) that displaces the substrate into the central cavity.

(C) Top views of open and closed crystal structures from Cpn (Pereira et al., 2010) highlighting the substrate-binding region (pink) and *rls* loop (green).

chains exposed in the closed state as well as the effect of crowding on the solvent properties of the chamber (Tang et al., 2006). The hetero-oligomeric nature of most group II chaperonins may lead to a diversification of the chamber properties (Cong et al., 2010), which may contribute to the folding of specific substrates. Although a single encapsulation step suffices for optimal folding in vitro, it is important to consider that in the cellular context, cycling on and off the chaperonin likely fulfills an important homeostatic function. Thus, each cycle may expose the substrate polypeptide to additional folding cofactors as well as quality control components, thereby preventing folding-incompetent proteins from clogging the chaperonin. How the balance between processivity and clearance is achieved in vivo is an important question for future research.

ATP Hydrolysis Triggers Substrate Release through a Unique Interdomain Displacement Mechanism

ATP hydrolysis releases the bound substrate from its chaperonin-binding sites through a hitherto unanticipated mechanism; namely, a conformational change that brings together vicinal apical domains. This creates a lateral interface between helix 11 of one domain and loop 327–331 in the adjacent subunit (Figures 7B and 7C, pink and green, respectively). The crystal structure suggests that formation of this lateral H-bonded network is incompatible with substrate binding. We hypothesize that these lateral intersubunit contacts displace the substrate from its binding site (pink in Figure 7). The precise mechanism of release will require further investigation. One possibility is that the intersubunit interaction sterically interferes with substrate rebinding during thermal breathing of the chaperonin-substrate interaction. Alternatively, the helix 11-*rls* loop interaction could create an entropic zipper that displaces the substrate. Yet another model is that the *rls* interaction helps stabilize a conformation that cannot bind substrate. The presence of ATP•AlFx may compensate energetically for the loss of the H-bonded network between substrate-binding region and *rls* loop, and by itself induce the subtle conformational change required to release the substrate.

The unique nature of substrate release in group II chaperonins may have important implications for hetero-oligomeric chaperonins, particularly in light of recent findings that different subunits recognize distinct motifs in the substrate (Spiess et al., 2006). Because the mechanism for substrate release depends on the nature of a specific intersubunit interface, rather than a general GroES-binding interface as observed in GroEL, the local kinetics of substrate release could vary for a specific apical domain (e.g., shading in Figure 7B). The order of release of different regions of a substrate polypeptide from their respective subunits may be influenced by the strength of this interaction vis-à-vis the timing of conformational change and formation of the lateral interface. The ensuing sequential mechanism of substrate release from the chaperonin could provide exquisite control of the folding pathway of the substrate, which in turn contributes to the unique ability of these chaperonins to fold specific proteins. One could envision that subunit-specific substrate remodeling and/or ordered release directs substrates of group II chaperonins along specific folding trajectories. Exploring these exciting possibilities may have profound implications for our understanding and ability to control cellular folding pathways.

EXPERIMENTAL PROCEDURES

Biochemical Approaches

All Cpn variants were produced by site-directed mutagenesis; purification and functional analyses were performed as described (Reissmann et al., 2007). MDH refolding was performed as in Hayer-Hartl (2000). Fluorescent proteins were generated as in Kim et al. (2005), and fluorescence was measured on a FluoroLog-3 Fluorometer (HORIBA Jobin Yvon).

Cryo-EM Analyses

Samples were embedded in vitreous ice on 400-mesh R1.2/1.3 Quantifoil grids (Quantifoil Micro Tools GmbH, Jena Germany) and imaged on a JEM3200FSC electron cryo-microscope and JEM2010F electron cryo-microscope (JEOL Ltd., Tokyo, Japan) with field emission guns. Details about the image acquisition parameters are in Table S1 of the Extended Experimental Procedures. The image processing steps followed those described in (Baker et al., 2010). The figures were prepared using MacPyMOL (http://www.pymol.org) and UCSF Chimera (Pettersen et al., 2004).

ACCESSION NUMBERS

Coordinates have been deposited in the Electron Microscopy Databank and Protein Data Bank under ID codes EMD-5244, PDB:3IZH; EMD-5245, PDB:3IZI; EMD-5246, PDB:3IZJ; EMD-5247, PDB:3IZK; EMD-5248, PDB:3IZL; EMD-5249, PDB:3IZM; and EMD-5250, PDB:3IZN.

SUPPLEMENTAL INFORMATION

Supplemental Information includes Extended Experimental Procedures, five figures, and one table and can be with this article online at doi:10.1016/j.cell.2010.12.017.

ACKNOWLEDGMENTS

We thank Dr. W.E. Moerner for providing Nile Red maleimide and advice on fluorescence microscopy. We also thank members of the J.F. laboratory and Raul Andino for critical reading of the manuscript; Frank DiMaio and David Baker for advice on modeling; Erik Miller for useful discussions; and Jeremy England and Erik Miller for providing PepB. This work was supported by NIH Grants GM74074 (to J.F.), 5PN2EY016525 (to J.F. and W.C.), and P41RR002250 (to W.C.). N.R.D. was a recipient of predoctoral ARCS fellowships and was supported by an NIH training grant (T32-007276). J.Z. was a recipient of NIH training grants on nanobiology (R90 DK071054 and T90 DA022885).

Received: July 21, 2010
Revised: October 26, 2010
Accepted: December 10, 2010
Published: January 20, 2011

REFERENCES

Baker, M.L., Zhang, J., Ludtke, S.J., and Chiu, W. (2010). Cryo-EM of macromolecular assemblies at near-atomic resolution. Nat. Protoc. *5*, 1697–1708.

Bigotti, M.G., and Clarke, A.R. (2005). Cooperativity in the thermosome. J. Mol. Biol. *348*, 13–26.

Bigotti, M.G., and Clarke, A.R. (2008). Chaperonins: the hunt for the group II mechanism. Arch. Biochem. Biophys. *474*, 331–339.

Bigotti, M.G., Bellamy, S.R., and Clarke, A.R. (2006). The asymmetric ATPase cycle of the thermosome: elucidation of the binding, hydrolysis and product-release steps. J. Mol. Biol. *362*, 835–843.

Booth, C.R., Meyer, A.S., Cong, Y., Topf, M., Sali, A., Ludtke, S.J., Chiu, W., and Frydman, J. (2008). Mechanism of lid closure in the eukaryotic chaperonin TRiC/CCT. Nat. Struct. Mol. Biol. *15*, 746–753.

Clare, D.K., Stagg, S., Quispe, J., Farr, G.W., Horwich, A.L., and Saibil, H.R. (2008). Multiple states of a nucleotide-bound group 2 chaperonin. Structure *16*, 528–534.

Cong, Y., Baker, M.L., Jakana, J., Woolford, D., Miller, E.J., Reissmann, S., Kumar, R.N., Redding-Johanson, A.M., Batth, T.S., Mukhopadhyay, A., et al. (2010). 4.0-A resolution cryo-EM structure of the mammalian chaperonin TRiC/CCT reveals its unique subunit arrangement. Proc. Natl. Acad. Sci. USA *107*, 4967–4972.

DiMaio, F., Tyka, M.D., Baker, M.L., Chiu, W., and Baker, D. (2009). Refinement of protein structures into low-resolution density maps using rosetta. J. Mol. Biol. *392*, 181–190.

Ditzel, L., Löwe, J., Stock, D., Stetter, K., Huber, H., Huber, R., and Steinbacher, S. (1998). Crystal structure of the thermosome, the archaeal chaperonin and homolog of CCT. Cell *93*, 125–138.

Frydman, J. (2001). Folding of newly translated proteins in vivo: the role of molecular chaperones. Annu. Rev. Biochem. *70*, 603–647.

Frydman, J., and Hartl, F.U. (1996). Principles of chaperone-assisted protein folding: differences between in vitro and in vivo mechanisms. Science *272*, 1497–1502.

Gómez-Puertas, P., Martín-Benito, J., Carrascosa, J.L., Willison, K.R., and Valpuesta, J.M. (2004). The substrate recognition mechanisms in chaperonins. J. Mol. Recognit. *17*, 85–94.

Hartl, F.U., and Hayer-Hartl, M. (2009). Converging concepts of protein folding in vitro and in vivo. Nat. Struct. Mol. Biol. *16*, 574–581.

Hayer-Hartl, M. (2000). Assay of malate dehydrogenase. A substrate for the *E. coli* chaperonins GroEL and GroES. Methods Mol. Biol. *140*, 127–132.

Iizuka, R., Yoshida, T., Shomura, Y., Miki, K., Maruyama, T., Odaka, M., and Yohda, M. (2003). ATP binding is critical for the conformational change from an open to closed state in archaeal group II chaperonin. J. Biol. Chem. *278*, 44959–44965.

Kanzaki, T., Iizuka, R., Takahashi, K., Maki, K., Masuda, R., Sahlan, M., Yebenes, H., Valpuesta, J.M., Oka, T., Furutani, M., et al. (2008). Sequential action of ATP-dependent subunit conformational change and interaction between helical protrusions in the closure of the built-in lid of group II chaperonins. J. Biol. Chem. *283*, 34773–34784.

Kim, S., Semyonov, A., Twieg, R., Horwich, A., Frydman, J., and Moerner, W. (2005). Probing the sequence of conformationally induced polarity changes in the molecular chaperonin GroEL with fluorescence spectroscopy. J. Phys. Chem. B *109*, 24517–24525.

Llorca, O., Martín-Benito, J., Grantham, J., Ritco-Vonsovici, M., Willison, K., Carrascosa, J., and Valpuesta, J. (2001). The 'sequential allosteric ring' mechanism in the eukaryotic chaperonin-assisted folding of actin and tubulin. EMBO J. *20*, 4065–4075.

Martin, J., Langer, T., Boteva, R., Schramel, A., Horwich, A., and Hartl, F. (1991). Chaperonin-mediated protein folding at the surface of groEL through a 'molten globule'-like intermediate. Nature *352*, 36–42.

Meyer, A.S., Gillespie, J.R., Walther, D., Millet, I.S., Doniach, S., and Frydman, J. (2003). Closing the folding chamber of the eukaryotic chaperonin requires the transition state of ATP hydrolysis. Cell *113*, 369–381.

Pereira, J.H., Ralston, C.Y., Douglas, N., Meyer, D., Knee, K.M., Goulet, D.R., King, J.A., Frydman, J., and Adams, P.D. (2010). Crystal structures of a group II chaperonin reveal the open and closed states associated with the protein folding cycle. J. Biol. Chem. *285*, 27958–27966.

Pettersen, E.F., Goddard, T.D., Huang, C.C., Couch, G.S., Greenblatt, D.M., Meng, E.C., and Ferrin, T.E. (2004). UCSF Chimera—a visualization system for exploratory research and analysis. J. Comput. Chem. *25*, 1605–1612.

Powers, E.T., Morimoto, R.I., Dillin, A., Kelly, J.W., and Balch, W.E. (2009). Biological and chemical approaches to diseases of proteostasis deficiency. Annu. Rev. Biochem. *78*, 959–991.

Reissmann, S., Parnot, C., Booth, C.R., Chiu, W., and Frydman, J. (2007). Essential function of the built-in lid in the allosteric regulation of eukaryotic and archaeal chaperonins. Nat. Struct. Mol. Biol. *14*, 432–440.

Spiess, C., Meyer, A., Reissmann, S., and Frydman, J. (2004). Mechanism of the eukaryotic chaperonin: protein folding in the chamber of secrets. Trends Cell Biol. *14*, 598–604.

Spiess, C., Miller, E., McClellan, A., and Frydman, J. (2006). Identification of the TRiC/CCT substrate binding sites uncovers the function of subunit diversity in eukaryotic chaperonins. Mol. Cell *24*, 25–37.

Stuart, S.F., Leatherbarrow, R.J., and Willison, K.R. (2011). A two-step mechanism for the folding of actin by the yeast cytosolic chaperonin. J. Biol. Chem. *286*, 178–184.

Tang, Y.C., Chang, H.C., Roeben, A., Wischnewski, D., Wischnewski, N., Kerner, M.J., Hartl, F.U., and Hayer-Hartl, M. (2006). Structural features of the GroEL-GroES nano-cage required for rapid folding of encapsulated protein. Cell *125*, 903–914.

Thulasiraman, V., Yang, C., and Frydman, J. (1999). In vivo newly translated polypeptides are sequestered in a protected folding environment. EMBO J. *18*, 85–95.

Villebeck, L., Persson, M., Luan, S.L., Hammarstrom, P., Lindgren, M., and Jonsson, B.H. (2007). Conformational rearrangements of tail-less complex polypeptide 1 (TCP-1) ring complex (TRiC)-bound actin. Biochemistry *46*, 5083–5093.

Yam, A.Y., Xia, Y., Lin, H.T., Burlingame, A., Gerstein, M., and Frydman, J. (2008). Defining the TRiC/CCT interactome links chaperonin function to stabilization of newly made proteins with complex topologies. Nat. Struct. Mol. Biol. *15*, 1255–1262.

Zhang, J., Baker, M.L., Schroder, G.F., Douglas, N.R., Reissmann, S., Jakana, J., Dougherty, M., Fu, C.J., Levitt, M., Ludtke, S.J., et al. (2010). Mechanism of folding chamber closure in a group II chaperonin. Nature *463*, 379–383.